Nuclear Physics **A399** (1983) 230–240

ACCURATE DETERMINATION OF THE ^{17}O-^{16}O+n COUPLING CONSTANT AND SPECTROSCOPIC FACTOR

S. BURZYNSKI†, M. BAUMGARTNER, H. P. GUBLER, J. JOURDAN, H. O. MEYER, G. R. PLATTNER, H. W. ROSER and I. SICK

Department of Physics, University of Basel, 4056 Basel, Switzerland

and

K. -H. MÖBIUS

Max Planck-Institut für Kernphysik, Heidelberg, Germany

Received 13 October 1982
(Revised 29 November 1982)

We have measured ^{16}O-^{17}O elastic cross sections at 22 MeV between 65°-140° to ±1 %. The observed oscillatory interference between Coulomb scattering and the neutron transfer process is analyzed using exact finite-range DWBA. A model-independent value of $\bar{C}^2 = 0.82 \pm 0.07$ is obtained for the coupling constant of the $1d_{\frac{5}{2}}$ neutron in ^{17}O. We also present an analysis of data on magnetic electron scattering from ^{17}O, which yields precise information on the magnitude and the radial shape of the $1d_{\frac{5}{2}}$ neutron bound-state wave function. With this we relate the coupling constant to the spectroscopic factor and find $S = 1.06 \pm 0.11$. We show that the magnetic electron scattering data alone yield $S = 1.04 \pm 0.10$. Combining these results with earlier work we recommend $\bar{C}^2 = 0.79 \pm 0.04$ and $S = 1.03 \pm 0.07$ as best values. This spectroscopic strength corresponds to (91 ± 7) % of the full single-particle value.

E | NUCLEAR REACTIONS ^{16}O(^{17}O, ^{17}O), $E = 22$ MeV; measured $\sigma(\theta)$; deduced $d_{5/2}$ neutron coupling constant. Exact finite-range DWBA analysis. ^{17}O(e, e), E not given; analyzed data; deduced neutron wave function. ^{17}O deduced absolute S.

1. Introduction

The present paper describes the accurate determination of the $1d_{\frac{5}{2}}$ spectroscopic factor in ^{17}O by ^{16}O-^{17}O elastic scattering. This work is very similar in method and spirit to an investigation of the $1p_{\frac{1}{2}}$ neutron spectroscopic factor in ^{13}C by ^{12}C-^{13}C elastic scattering, published five years ago by our group [1]). There we studied the interference between direct and neutron-exchange contributions to

† On leave from the Institute of Nuclear Research, Poland.

elastic scattering at interaction energies below the Coulomb barrier. We showed that in this manner the neutron radial wave function at large radii and – with additional information obtained from electron scattering – the neutron spectroscopic factor can be precisely determined, free of the usual ambiguities caused by the poorly known nuclear interaction. We invite the interested reader to refer to that paper [1]) for a more detailed description of the method and its particular advantages. Here we shall mainly emphasize those aspects which differ from the earlier work. In a separate section (sect. 5) we present an analysis of existing data on magnetic electron scattering from ^{17}O. This yields both an independent value of the neutron spectroscopic factor and information on the shape of the neutron wave function, needed for the analysis of the neutron transfer contribution to ^{16}O-^{17}O elastic scattering.

2. Experimental procedure

We have measured the relative differential cross section of ^{16}O-^{17}O elastic scattering at c.m. angles between 67° and 136° in steps of approximately 1.5° at a c.m. energy of 10.6 MeV, i.e. at a ^{17}O bombarding energy of 22 MeV. The experiment was carried out at the Heidelberg EN Tandem Van de Graaff accelerator. A scattering chamber with 50 cm diameter housed the target and a set of four detectors in a particular arrangement as described below. The beam was tightly collimated by a 1.0×1.5 mm^2 slit situated 50 cm upstream from the target. The four blades of the slit were electrically insulated, so that the fraction of beam lost on each could be monitored. The beam was kept centered on this slit at all times. After passing through the target, where it had a diameter of approximately 1 mm, the beam was intercepted 35 cm downstream by a "split" Faraday cup, which again allowed to keep the beam positioned to within ± 0.5 mm. Thus, the angular displacement of the beam was limited to less than $\pm 0.07°$.

The target consisted of 20 μg/cm^2 Al_2O_3 evaporated onto a 10 μg/cm^2 self-supporting C-foil. The scattered particles were detected by a pair of silicon surface-barrier detectors mounted on a movable arm in a coincidence arrangement, by which unwanted background events could be virtually eliminated (e.g. inelastic events, contaminants, etc.).

Detector 1 with an entrance slit of 2×3 mm^2 at a distance of 175 mm from the target (angular resolution $\pm 0.33°$) served to measure the energy E_1 of a scattered ^{17}O (recoiling ^{16}O), while the companion detector 2 measured *in coincidence* the associated recoiling ^{16}O (scattered ^{17}O). This detector was position-sensitive, recording both the energy E_2 and the precise scattering angle θ_2 of the associated particle. It was positioned at 42 mm from the target, carried a 10×6 mm^2 slit and was always kept at an angle of 87.5° relative to detector 1, as dictated by the kinematics of ^{16}O–^{17}O elastic scattering.

When a particle is detected in a precisely defined direction by detector 1, the associated particle's direction is only constrained to lie within a finite cone, determined by the beam divergence and multiple scattering effects, which tend to smear out the strict kinematical correlations. We have carefully verified that the angular acceptance of detector 2 was large enough to permit the detection of more than 99.5 % of all correlated events.

For normalization purposes and to monitor beam displacements, scattered particles were also detected at $\theta_{lab} = \pm 15°$ by a symmetrically positioned pair of monitor surface-barrier detectors. For every run we checked that the left-right asymmetry of the monitor count rates stayed within ± 2 % of the mean value, corresponding to a maximal angular beam shift of $\pm 0.04°$. The accuracy in the position of the moveable detector mount being better than $\pm 0.1°$, the total uncertainty of the scattering angle was approximately $\pm 0.1°$. This precision was sufficient to keep the influence of the strong angular variation of the cross section below ± 1 %.

The beam current was kept at about 50 nA of $^{17}O^{4+}$. The deadtime losses in the ADC units were measured by using a pulser. A corresponding correction (never exceeding a few percent) was applied to the data.

The events, characterized by the three parameters E_1, E_2 and θ_2, in addition to the angle setting θ_1 of the principal detector, were stored on magnetic tape. The data analysis was done off-line. Both elastically scattered ^{17}O as well as recoil ^{16}O nuclei were considered when evaluating the scattering cross section. The analysis consisted in defining an optimal projection in the three-dimensional (E_1, E_2, θ_2) space onto an axis (defined as a linear combination of the three parameters) along which the best separation of ^{17}O and ^{16}O was achieved. Contributions from unwanted reactions (inelastic scattering, target contaminants aso) could easily be separated on the basis of their differing kinematics. The two peaks in the resulting one-dimensional spectra generally showed a peak-to-valley ratio of about 10. They were integrated directly. The overlap corrections were mostly of the order of a few percent and were determined by fitting appropriate peak shapes to the spectra.

The c.m. cross sections obtained from scattered ^{17}O and recoiling ^{16}O ions agreed within the error bars of $\approx \pm 1$ %. The errors are mainly statistical with the exception of the back-angle region, where the disproportionate sizes of the scattered and recoil peaks led to increased errors of up to ± 8 %.

The relative normalization of the cross sections was obtained using the monitor detectors at $\theta_{lab} = 15°$. Their count-rate was determined by integrating the huge elastic scattering peak in their energy spectra. An absolute normalization of the data was not attempted. Considerations of target thickness, beam current and detector solid angles lead to a rough normalization only, with an uncertainty of at least ± 50 %. We wish to emphasize, however, that the absolute normalization of our data enters as a higher order effect only into the extraction of the $^{17}O - ^{16}O + n$ spectroscopic factor.

It may be useful to note that we made two earlier attempts to measure such accurate sub-Coulomb ^{16}O-^{17}O cross sections. We scattered ^{17}O ions from a thin ^{16}O gas target and detected direct as well as recoiling particles as singles in a position-sensitive detector subtending the full angular region of interest on one side of the beam. Both attempts failed as evidenced by a $\sim 5\,\%$ disagreement between the c.m. cross sections obtained from scattered and recoiling particles. In retrospect we can attribute these failures to the presence of a few percent inelastic contribution, which we could not eliminate because of the insufficient resolution of the Si detector for such low-energy ions.

3. Theory

The description of the elastic scattering process ^{16}O(^{17}O, ^{17}O)^{16}O must contain amplitudes corresponding both to elastic potential scattering and to the elastic transfer reaction [e.g. ref. [2])].
Thus

$$\frac{\mathrm{d}\sigma}{\mathrm{d}\Omega}(\theta) = |f^{\mathrm{el}}(\theta) + f^{\mathrm{tr}}_{l=0}(\pi-\theta)|^2 + \sum_{l=1}^{4} |f^{\mathrm{tr}}_{l}(\pi-\theta)|^2, \tag{1}$$

where θ denotes the c.m. scattering angle. For the transfer of a $\mathrm{d}_{\frac{5}{2}}$ particle it is found that the transferred angular momentum l can vary between $0 \leqq l \leqq 4$. Only the $l = 0$ transfer interferes coherently with the direct scattering process. The amplitudes corresponding to transferred angular momenta $1 \leqq l \leqq 4$ must each be added incoherently.

We have calculated the transfer amplitudes in exact finite-range distorted-wave Born approximation [EFR DWBA, computer code LOLA [3])] including all Coulomb interaction terms [4]). The transfer amplitudes are proportional to SN^2, where S is the spectroscopic factor of the $1\mathrm{d}_{\frac{5}{2}}$ neutron in ^{17}O and N the asymptotic normalization of the corresponding bound-state wave function with unit modulus

$$\psi_{\frac{5}{2}}(\boldsymbol{r}) = R(r)Y_{2m}(\hat{\boldsymbol{r}}), \tag{2}$$

$$R(r) \to N\kappa h_2(i\kappa r) \qquad \text{for} \qquad r \to \infty. \tag{3}$$

The symbol h_2 denotes the Hankel function of the second kind [5]), $i\kappa = 0.4337i$ fm^{-1} is the wave number for the $1\mathrm{d}_{\frac{5}{2}}$ bound state in ^{17}O and r is the distance between the neutron and the ^{16}O core. A quantity commonly used is also the asymptotic norm or *coupling constant* [6])

$$\bar{C}^2 = (2\kappa)^{-1} SN^2. \tag{4}$$

It enters linearly into the interference terms of $f^{el}(\theta)$ with $f^{tr}_{l=0}(\pi-\theta)$. Since the incoherent transfer contributions are small and vary smoothly with angle, $\bar{C}^2$ can be determined quite accurately [1]) from the amplitude of the interference pattern †.

4. Analysis

We have determined a large number of optical potentials which, together with the transfer contribution, fit the measured angular distribution of the cross section. These potentials consist of a real plus an imaginary part with a variety of form factors. For the real part we tried "volume" terms (i.e. standard Woods-Saxon form factor), "surface" terms (i.e. 1st derivative of a WS shape) and 2nd derivative terms which mimic the "peripheral attraction-central repulsion" characteristic of microscopic potentials [e.g. ref. [7])]. For the imaginary part a "surface" term was taken, with one exception. Table 1 lists the potentials used in the analysis. Large variations in the choice of the potential parameters are possible. We note that some of the potentials have shallow real parts as predicted by the folding model [7,8]). The best fit value of the coupling constant $\bar{C}^2$ and χ^2 per point are also indicated.

The experimental data – normalized for best fit – and the EFR DWBA cross section are shown in fig. 1. The agreement between data and calculation is excellent. All of the potentials listed in table 1 yield results which to the eye are indistinguishable from those presented in fig. 1. The average of the $\bar{C}^2$ values in table 1 is taken as the result of our analysis, with an uncertainty chosen such as to include the extremes. This yields

$$\bar{C}^2 = 0.82 \pm 0.07.$$

This error is meant to represent the uncertainty of the analysis. The purely statistical error is much smaller.

The quoted error does not contain possible systematic shortcomings of the EFR DWBA theory, the most obvious of which is the neglect of coupling to the $2s_{\frac{1}{2}}$ first excited state of ^{17}O. For direct elastic scattering such coupled channel effects are incorporated in the empirical effective optical potential. To estimate this influence on the elastic transfer process we can use results obtained in a detailed study by Baur and Wolter [9]) of multistep transfer processes in ^{16}O-^{17}O inelastic scattering. We find that at $\theta_{c.m.} = 90°$, near the peak of the inelastic cross section, the coupling to the $2s_{\frac{1}{2}}$ state yields an additional (two-step) elastic transfer amplitude with a magnitude of $\sim 1\ \%$ of the direct elastic scattering amplitude. Only its $l = 0$ transfer part contributes coherently to the (uncoupled, one-step) transfer amplitude

† Note that according to these definitions, the quantity C in ref. [1]) should also be called $\bar{C}$.

TABLE 1

Nuclear optical potentials for $^{17}O+^{16}O$

V_R (MeV)	r_{0R} (fm)	a_R (fm)	f_R	V_I (MeV)	r_{0I} (fm)	a_I (fm)	f_I	χ^2/N	$\bar{C}^2$
91.8	1.04	0.67	g	17.1	1.14	0.71	g'	1.4	0.75
44.8	1.17	0.67	g	43.5	1.20	0.43	g'	1.4	0.88
28.6	1.35	0.38	g'	33.6	0.95	0.73	g'	1.5	0.87
15.7	1.38	0.50	g	4.2	0.92	1.07	g'	1.5	0.88
33.1	1.16	0.75	g''	22.4	1.48	1.20	g'	1.7	0.84
205.2	0.88	0.74	g	29.1	1.28	0.47	g'	1.7	0.75
10.5	1.26	0.90	g	40.5	1.30	0.36	g'	1.7	0.80
24.8	1.32	0.65	g'	71.9	1.41	0.21	g'	1.7	0.82
10.4	1.23	0.90	g	2.9	1.56	0.25	g	1.7	0.80
10.0	1.41	0.73	g''	66.4	1.18	0.48	g'	1.8	0.80
59.3	0.70	1.15	g''	15.1	1.44	0.25	g'	1.8	0.79

$U_{opt} \equiv V_C - V_R f_R - iV_I f_I, \quad g(x_i) = [1+\exp(x_i)]^{-1}, \quad x_i = (r-R_i)/a_i, \quad R_i = r_{0i}(A_1^{\frac{1}{3}}+A_2^{\frac{1}{3}}).$

from which we determine the coupling constant $\bar{C}^2$ (see eq. (1)). As a consequence, the effect of this higher-order contribution on our result is further strongly reduced to an estimated 0.05 % of the direct elastic or 1 % of the coherent one-step elastic transfer amplitude, well within the error quoted above.

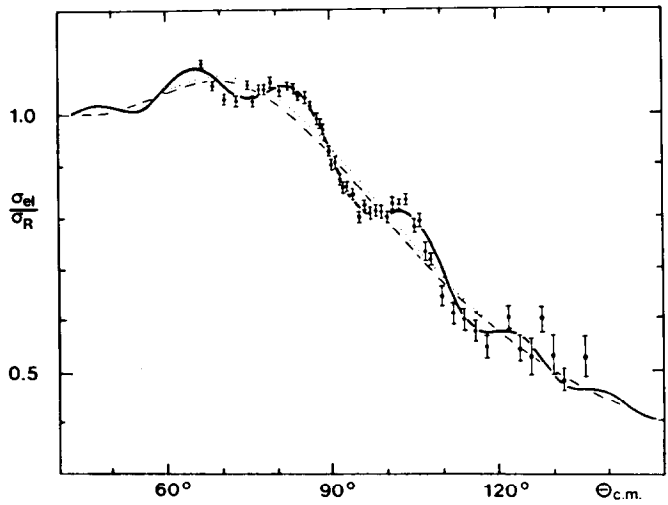

Fig. 1. Differential cross section of $^{16}O(^{17}O, ^{17}O)^{16}O$ at $E_{c.m.} = 10.6$ MeV. The overall normalization of the data is chosen to give optimal agreement with the EFR DWBA calculation represented by the full line, which includes the elastic transfer process in all transferred angular momentum states. The dashed line indicates the corresponding potential scattering, the dotted line represents potential scattering plus the incoherent contributions of the transferred angular momenta $1 \leqq l \leqq 4$.

The potential well used to calculate the $1d_{\frac{5}{2}}$ neutron bound-state wave function is given by a standard Woods-Saxon well with a surface spin-orbit term, as described in our earlier paper [1]). The following parameters were taken as representative of the empirical information on the n-^{16}O interaction obtained from magnetic electron scattering (see sect. 5 below): $V = 53.1$ MeV (adjusted to reproduce the neutron separation energy in ^{17}O), $r_0 = 0.882 \pm 0.016$ fm, $a = 0.600$ fm, $\lambda_{s.o.} = 24$. This leads to an asymptotic normalization constant $N = 0.817 \pm 0.021$ fm$^{-\frac{1}{2}}$. Thus we obtain from eq. (4) for the ^{17}O-^{16}O+n spectroscopic factor a value of

$$S = 1.06 \pm 0.11$$

from the data on ^{16}O-^{17}O elastic scattering presented in this paper. It should be stressed that the choice of bound-state wave function does not appreciably affect the value of $\bar{C}^2$ extracted from the data [1]). The value of S related to a given value of $\bar{C}^2$ depends very strongly on that choice, however. In particular, a 1 % change of the radius parameter r_0 leads to a 5 % change of S for a fixed coupling constant $\bar{C}^2$. Thus, great care must be taken to determine a realistic bound-state wave function.

5. Magnetic electron scattering

In order to obtain a spectroscopic factor S from a known coupling constant $\bar{C}^2$, independent information on the radial shape of the wave function is required. In this section we present an analysis of recent data [10]) on magnetic electron scattering from ^{17}O, which determines the shape and radius of the $1d_{\frac{5}{2}}$ neutron wave function with good precision and which in itself provides independent information on S.

Elastic electron scattering from ^{17}O is very sensitive to the $1d_{\frac{5}{2}}$ neutron orbit, which is mainly responsible for the radial distribution of the magnetization. In particular, the form factor of the highest allowed multipolarity, M5, for the shell of highest spin can be interpreted without ambiguity in terms of the radial distribution of the neutron. For a detailed discussion of the merits and the sensitivity of the method the reader is referred to the work of Platchkov *et al.* [11]) and to the references cited therein. For a favourable case such as ^{17}O a precision of 1 % in the radius of the neutron orbit can be expected.

The data of Hynes *et al.* [10]) cover a momentum transfer range 0.5 fm$^{-1} < q < 2.8$ fm^{-1} and are dominated by the M1 and M5 contributions to low and high q, respectively. Hynes *et al.* [10]) have already converted the electron scattering cross sections to PWBA form factors by using a DWBA code. We have corrected the data for the contribution of meson-exchange currents (MEC) as calculated by Suzuki *et al.* [12]).

We have parametrized the radial neutron wave function by a calculation using a Woods-Saxon well with surface thickness $a = 0.6$ fm and a spin-orbit parameter [1] $\lambda_{s.o.} = 24$. The radius parameter r_0 was fitted to the magnetic scattering data. The magnetic scattering form factors were calculated in PWBA using a computer code developed by Donnelly and Sick [13]. The overall amplitudes α_λ of the different multipolarities λ were treated as additional parameters. Center-of-mass corrections and the finite neutron size were taken into account as in ref. [11]).

The best fit to the magnetic form factor data is shown in fig. 2. The χ^2 is 6 for 12 degrees of freedom, the radius parameter [quoted as in ref. [1]) according to $R_{WS} = (16^{\frac{1}{3}} + 1)r_0$] is $r_0 = 0.838 \pm 0.015$ fm and the strength for $\lambda = 5$ amounts to $\alpha_5 = 0.92 \pm 0.09$. The corresponding rms radius of the $1d_{\frac{5}{2}}$ neutron wave function is 3.35 ± 0.03 fm. The quoted errors include estimates of the systematic uncertainties of the data, the MEC correction and the effect of configuration mixing. Contrary to the conclusion reached in ref. [10]), we find that the magnetic form factor can be well explained by assuming a reasonable neutron wave function, the radial extent of which moreover agrees well with a Renormalized Brueckner calculation by Vary *et al.* [19]).

In order to use this information on the neutron orbit in our analysis of the neutron-transfer contribution to ^{16}O-^{17}O scattering, we must perform a change of coordinate systems. The magnetic form factors are calculated using a shell-model wave function with a radius parameter r' corresponding to the distance between the neutron and the potential origin. The transfer reaction, on the other hand, is analyzed in an intrinsic coordinate r that refers to the distance between the

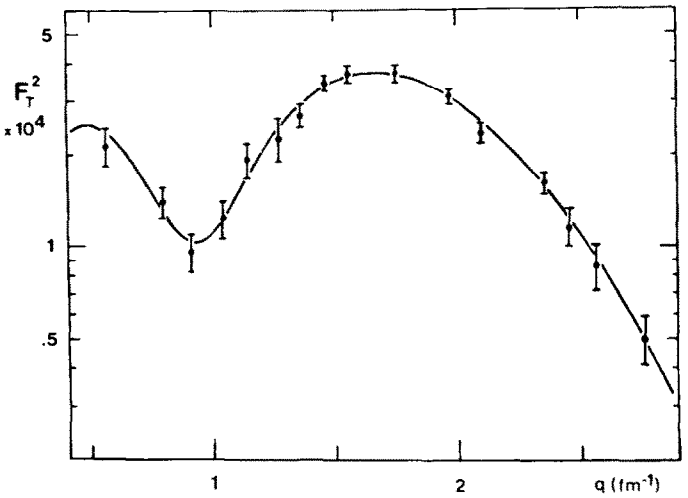

Fig. 2. The magnetic electron-scattering form factor for $^{17}O(e, e)^{17}O$. The data are taken from ref. [10]). The full line represents our calculation using a $1d_{\frac{5}{2}}$ neutron wave function generated by the Woods-Saxon potential indicated in the text (sect. 5).

neutron and the ^{16}O core (see sect. 4). The ratio r/r' can be calculated for the HO shell model [14]) and is obtained as $r/r' = \sqrt{A/(A-1)} = 1.031$. Thus, to analyze the neutron transfer process we must increase the rms radius of the bound state potential by a factor of 1.031. This is achieved – leaving the surface thickness fixed – by increasing the radius parameter to $r_0 = 0.882 \pm 0.016$ fm. This is the value used in sect. 4 to generate the bound-state wave function of the $1d_{\frac{5}{2}}$ neutron. To the extent that no significant $l = 2$ strength to states other than the ground state of ^{16}O has been observed [15]) in ^{17}O(p, d)^{16}O, our value for α_5 yields the $1d_{\frac{5}{2}}$ spectroscopic factor and – in conjunction with the neutron wave function – also the coupling constant $\bar{C}^2$. We must again convert from the shell-model frame to the intrinsic frame. As shown by Clement [16]) this requires a multiplication of α_5 by $(A/(A-1))^2 = 1.13$, a quantity which represents the maximal spectroscopic factor of one unpaired $1d_{\frac{5}{2}}$ neutron. Thus, we find that the magnetic electron scattering experiment alone yields a spectroscopic factor for the $1d_{\frac{5}{2}}$ neutron in ^{17}O of

$$S = 1.04 \pm 0.10,$$

or, from eq. (4), a coupling constant

$$\bar{C}^2 = 0.80 \pm 0.08.$$

6. Discussion

Recent accurate values of $\bar{C}^2$ are compiled in table 2. Cooper *et al.* [17]) have performed a careful DWBA study of the ^{16}O(d, p)^{17}O reaction at energies between 25 and 65 MeV. To compare their results to ours we have corrected their values to account for the slightly different bound-state wave function used. The value for $\bar{C}^2$ quoted in table 2 is the weighted mean and rms error of their six results, obtained at 3 different energies with 2 different sets of distorting d- and p-nucleus potentials.

Franey *et al.* [18]) have studied neutron transfer reactions on ^{208}Pb initiated with ^{12,13}C and ^{16,17}O projectiles, and also the ^{12}C(^{17}O, ^{16}O)^{13}C reaction. Apart from other information, they deduced coupling constants $\bar{C}^2$ for the $1p_{\frac{1}{2}}$ neutron in ^{13}C and for the $1d_{\frac{5}{2}}$ neutron in ^{17}O. Their value for ^{13}C agreed exactly with our earlier result for that nucleus [1, 6]). To compare their result for ^{17}O with ours we have again corrected their values to take the slight difference between the bound-state wave functions into account.

Both results [17, 18]) for the ^{17}O-^{16}O+n coupling constant agree very well with our evaluations, which agree perfectly among each other. Since the methods used to determine these 4 values are quite different, completely independent and of comparable accuracy, it makes sense to take the weighted mean as a recommended value, which is also given in table 2.

TABLE 2

^{17}O-^{16}O+n coupling constant $\bar{C}^2$ and spectroscopic factor S in intrinsic frame

Reaction	Ref.	$\bar{C}^2$	S
$^{16}O(d, p)^{17}O$	Cooper *et al.* [17])	0.76 ± 0.08	0.99 ± 0.12
$^{12}C(^{17}O, ^{16}O)^{13}C$ $^{208}Pb(^{17}O, ^{16}O)^{209}Pb$ $^{208}Pb(^{16}O, ^{17}O)^{207}Pb$ $^{208}Pb(^{13}C, ^{12}C)^{209}Pb$ $^{208}Pb(^{12}C, ^{13}C)^{207}Pb$	Franey *et al.* [18])	0.77 ± 0.08	1.00 ± 0.12
$^{16}O(^{17}O, ^{17}O)^{16}O$	present work	0.82 ± 0.07	1.06 ± 0.11
$^{17}O(e, e)^{17}O$	present work	0.80 ± 0.08	1.04 ± 0.10
recommended value (weighted mean)		0.79 ± 0.04	1.03 ± 0.07
single-particle value [Clement [16])]			1.13

We assume that the bound-state wave function determined by our analysis of magnetic electron scattering provides a good description of the $1d_{\frac{5}{2}}$ neutron in ^{17}O. Thus we can (eq. (4)) deduce the spectroscopic factor S from the coupling constant $\bar{C}^2$. These values are also indicated in table 2.

7. Conclusion

From accurately measured ^{16}O-^{17}O elastic cross sections we have been able to determine the coupling constant $\bar{C}^2$ of the $1d_{\frac{5}{2}}$ neutron wave function in ^{17}O to within $\pm 9\ \%$ in a model-independent manner. Using an independent-particle bound-state wave function determined by a fit to magnetic electron scattering cross sections we deduce the corresponding spectroscopic factor S. The analysis of the magnetic electron scattering data alone also allows a determination of S (and hence of $\bar{C}^2$) to within $\pm 10\ \%$. Both sets of numbers are in perfect agreement. Combining our results with those obtained earlier from the $^{16}O(d, p)^{17}O$ and heavy-ion transfer reactions we derive recommended values of $\bar{C}^2 = 0.79 \pm 0.04$ and $S = 1.03 \pm 0.07$. This spectroscopic strength corresponds to $(91 \pm 7)\ \%$ of the full single-particle value.

The authors wish to thank Drs. A. E. L. Dieperink and P. Egelhof for helpful discussions.

References

1) H. P. Gubler, G. R. Plattner, I. Sick, A. Traber and W. Weiss, Nucl. Phys. **A284** (1977) 114
2) P. E. Hodgson, in Nuclear heavy ion reactions (Oxford University Press, 1978) p. 374

3) R. M. De Vries, Phys. Rev. **C8** (1973) 951
4) R. M. De Vries, G. R. Satchler and J. G. Cramer, Phys. Rev. Lett. **32** (1974) 1377
5) M. Abramowitz and I. A. Stegun, Handbook of mathematical functions (Dover, NY, 1965)
6) G. R. Plattner and R. D. Viollier, Nucl. Phys. **A365** (1981) 8
7) D. M. Brink and Fl. Stancu, Nucl. Phys. **A243** (1975) 175
8) Fl. Stancu and D. M. Brink, Nucl. Phys. **A270** (1976) 236
9) G. Baur and H. H. Wolter, Phys. Lett. **51B** (1974) 205
10) M. V. Hynes, H. Miska, B. Norum, W. Bertozzi, S. Kowalski, F. N. Rad, C. P. Sargent, T. Sasanuma, W. Turchinetz and B. L. Berman, Phys. Rev. Lett. **42** (1979) 1444
11) S. K. Platchkov, J. B. Bellicard, J. M. Cavedon, B. Frois, D. Goutte, M. Huet, P. Leconte, Phan Xuan-Ho, P. DeWitt-Huberts, L. Lapikas and I. Sick, Phys. Rev. **C25** (1982) 2318
12) T. Suzuki, thesis, University of Tokio, 1978;
A. Arima, Y. Horikawa, H. Hyuga and T. Suzuki, Phys. Rev. Lett. **40** (1978) 1001; **42** (1979) 1186
13) T. W. Donnelly and I. Sick, to be published
14) A. E. L. Dieperink and I. Sick, Phys. Lett. **109B** (1982) 1
15) R. Mendelson, J. C. Hardy, J. Cerny, Phys. Lett. **31B** (1970) 126;
G. Mairle, G. J. Wagner, P. Doll, K. T. Knöpfle and H. Breuer, Nucl. Phys. **A299** (1978) 39
16) C. F. Clement, Nucl. Phys. **A213** (1973) 469
17) M. D. Cooper, W. F. Hornyak and P. G. Roos, Nucl. Phys. **A218** (1974) 249
18) M. A. Franey, J. S. Lilley and W. R. Phillips, Nucl. Phys. **A324** (1979) 193
19) J. P. Vary, R. H. Belehrad and R. J. McCarthy, Phys. Rev. **C21** (1980) 1626